Chemistry and Physics of Lipids 225 (2019) 104802

Contents lists available at ScienceDirect

Chemistry and Physics of Lipids

journal homepage: www.elsevier.com/locate/chemphyslip

The relationship between microwave radiation injury and abnormal lipid metabolism

Ying Tian, Ziming Xia, Min Li, Guangjie Zhang, Huimin Cui, Bin Li, Hongmei Zhou, Junxing Dong*

Department of Pharmaceutical Sciences, Beijing Institute of Radiation Medicine, Beijing 100850, PR China

ARTICLE INFO

Keywords:
Microwave radiation
Lipid metabolism
UPLC-MS
Linoleic acid
Glycerophospholipid
Glycerolipid

ABSTRACT

Microwave radiation can lead to some biological effects, mainly involving the nervous and reproductive systems. However, its lipid metabolic mechanism remains unclear. Here, we performed an untargeted metabolomics approach to analyze lipid metabolic changes caused by microwave radiation using ultra-performance liquid chromatography coupled with mass spectrometry (UPLC-MS). Then, multivariate analysis was used to reveal the different lipid metabolites and metabolic pathways. Compared with the sham group, biochemical parameters of the microwave group had significant changes in triglyceride (TG) and high-density lipoprotein (HDL) levels. Sixty-eight abnormal lipids were identified, which were mainly distributed in linoleic acid metabolism, glycerophospholipid metabolism, glycerolipid metabolism and glycosylphosphatidylinositol (GPI)-anchor biosynthesis. Among them, phosphatidylethanolamine (PE), lysophosphatidylethanolamine (LPE), lysophosphatidylcholine (LPC) and linoleic acid showed mainly upregulated expression, while sphingomyelin (SM), cholesterol esters (CE) and some free fatty acids (FFAs) showed downregulated expression. Phosphatidylcholine (PC) and triacylglycerol (TG) were increased or decreased. Furthermore, we obtained significant links between lipid metabolic changes and cognitive damage caused by microwave radiation. Together, our results suggested that microwave radiation could cause changes in lipid metabolism and provided a novel insight into the role of lipids in microwave radiation. Targeting lipid metabolism may provide a new therapeutic strategy for microwave radiation injury.

1. Instruction

Microwave radiation is nonionizing electromagnetic radiation (EMR) with a frequency range from 300 MHz to 300 GHz. Many electronic devices in daily use such as mobile phones, microwave ovens, radios, portable computers and television equipment, expose people to electromagnetic pollution and are associated with microwaves. Therefore, the effect of microwave radiation on human health has attracted increased attention (Redlarski et al., 2015).

Epidemiological investigation has indicated that microwave radiation as a health risk factor may cause microwave syndrome with such symptoms as fatigue, headache, insomnia, dysesthesia, irritability, and lack of concentration (Pall, 2016). Biological effects mainly focus on the central nervous system (Kaplan et al., 2016) and male sperm quality (Adams et al., 2014). Especially for the effects on the nervous system, there have been many investigations on molecular mechanisms, such as some signal pathways (Wang et al., 2014b; Zhao et al., 2014; Zuo et al., 2014a,b) and autophagy (Hao et al., 2018). Oxidative stress, induced by the excessive formation of reactive oxygen species (ROS), appears to be involved in the effect of microwave exposure (Chauhan et al., 2017; Yuksel et al., 2016) and as a potential therapeutic strategy for drug assay (Hu et al., 2014; Lewicka et al., 2017; Meena et al., 2014). In

Abbreviations: EMR, nonionizing electromagnetic radiation; ROS, reactive oxygen species; TAC, tricarboxylic acid cycle; UPLC-MS, ultra-performance liquid chromatography coupled with mass spectrometryt; SAR, special absorption rate; FDTD, finite-difference time-domain; MWM, Morris water maze; AEL, average escape latency; ALT, alanine aminotransferase; AST, aspartate aminotransferase; LDH, lactate dehydrogenase; CK, creatine kinase; TCHO, total cholesterol; TG, triacylglycerol or triglycerides; HDL, high-density lipoprotein; LDL, low-density lipoprotein; PCA, principal component analysis; OPLS-DA, orthogonal partial least squares discriminant analysis; VIP, variable importance in the projection; SD, standard deviation; CVs, coefficients of variation; PC, phosphatidylcholine; LPC, lysophosphatidylcholine; PE, phosphatidylethanolamine; LPE, lysophosphatidylethanolamine; FFA, free fatty acid; SM, sphingomyelin; CE, cholesterol esters; GPI, glycosylphosphatidylinositol; 9,10-EpOME, 9,10-epoxyoctadecamonoenoic acid; 9,10-DHOME, 9,10-dihydroxyoctadecamonoenoic acid

* Corresponding author.
E-mail address: djx931314@163.com (J. Dong).

https://doi.org/10.1016/j.chemphyslip.2019.104802
Received 4 April 2019; Received in revised form 3 July 2019; Accepted 28 July 2019
Available online 23 August 2019

addition, the contents of some biochemical parameters such as Ca^{2+}, CK and LDH, significantly increase due to microwave radiation (Zhang et al., 2017).

Recently, our study found an increase in the content of serum TG and a decrease in HDL in microwave-exposed rats. The results suggested that abnormal lipid metabolism could be closely related to microwave radiation. Wang et al. (2011) and Li et al. (2011) revealed that microwave exposure could cause the abnormality of tricarboxylic acid cycle (TAC) pathway metabolites, amino acids and monoamines involving mitochondrial function. However, there are still more questions than answers to fully understand the mechanism and metabolic change, especially the effects of lipids on microwave radiation injury.

Metabolomics has contributed to the understanding of different diseases and has been remarkably applied in disease diagnosis, mechanism elucidation and drug discovery. Ultra-performance liquid chromatography coupled with mass spectrometry (UPLC-MS) is a robust and reliable analytical approach with the high resolution of chromatographic peaks, increased analytic speed and sensitivity for complex mixtures. It is very suitable for the study of metabolomics and widely used to characterize the endogenous metabolic compounds of serum, plasma, urine and tissue (Zhao et al., 2012b, 2013a,b; Zhao and Lin, 2014). Thus, the present study was performed and intended to use an untargeted metabolomics approach to analyze whether microwave radiation could cause lipid metabolic changes and characteristics. We also investigated serum biochemistry data and cognitive behavior in rats to validate the disturbance of lipid metabolism induced by microwave radiation and explored the relationship between lipid metabolism and the biological effects of microwave radiation, which provides novel insight into the role of lipids in microwave radiation.

2. Materials and methods

2.1. Chemicals and reagents

HPLC-grade methanol, chloroform, isopropyl alcohol, acetonitrile and formic acid were purchased from Thermo Fisher Scientific (Pittsburgh, PA, USA). Ammonium acetate was obtained from Sigma-Aldrich (St. Louis, MO, USA) with 99% purity.

2.2. Experimental groups and exposure

Fifty male Wistar rats (180 ± 20 g) were obtained from the animal breeding center of Beijing Vital River Laboratories Company (Beijing, China) and were maintained at 22 ± 2 °C with a 12 h light-dark cycle. Food and water were freely available. All the procedures in this study were strictly performed according to the Guide for the Care and Use of Laboratory Animals. Rats were divided randomly into two groups, as follows: (1) Microwave radiation group (MW group, n = 25): animals were exposed to a 2.9 GHz generation system, which consisted of a pulse microwave generator (BZJ1500M-300W, Glory MV Electronics, China) and a 45 dB gain power amplifier (VE1079A, Beijing Vacuum Electronics Research Institute, China), for 15 min with an average power density of 30 mW/cm^2 daily for up to 3 days. The peak and average power densities were measured using a calibrated waveguide antenna, a power meter (N1912A, Keysight, USA) and an N1921 power sensor. The special absorption rate (SAR) was estimated by the software package Empire V5.10 based on the finite-difference time-domain (FDTD) method. The whole-body average SAR was 9.3 W/kg. Animals in the model groups were subjected to microwave exposure in individual polypropylene cages. (2) Sham group (SH group, n = 25): animals were handled and processed in parallel to the exposure groups but without microwave radiation.

2.3. Morris water maze (MWM) behavioral test

There were 10 rats in each group for the MWM behavioral test to evaluate learning and memory performance according to a previously reported method (Zhao et al., 2012a) after exposure to microwave radiation. Briefly, the test was performed in a circular pool with a diameter of 120 cm and a height of 50 cm filled with water at 23 ± 1 °C. The escape platform with a diameter of 12 cm was submerged 1 cm below the surface of the water. Before microwave radiation, the rats were guided to find the escape platform during 3 days of training (continuous and 4 trials per day). After microwave radiation, the trained rats were placed in the same start location and subjected to 4 trials with a maximum duration of 60 s for each trial. The behavior was digitally recorded by an MWM video analysis system (Beijing Zhongshidichuang Science and Technology Development Co. Ltd., Beijing, China), and the average escape latency (AEL) was used as the final index.

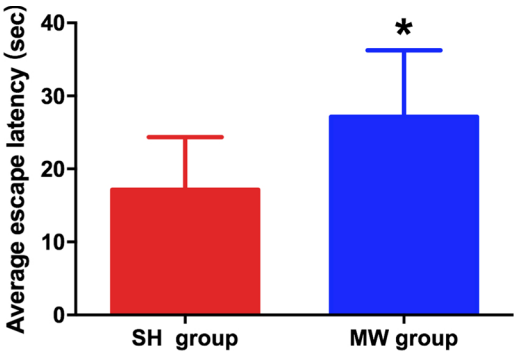

Fig. 1. MWM behavioral test in rats after microwave exposure 14 d. Data was shown as mean ± SD, * P < 0.05, compared with SH group.

2.4. Sample collection and lipid extraction

At 6 h, 7 d and 14 d after microwave exposure, blood samples of rats (n = 5) in each group drawn from the celiac vein were centrifuged at room temperature for 10 min at 1000 rpm. After centrifugation, serum samples were collected and immediately stored at −80 °C until used for biochemical analysis and lipid metabolic analysis.

The serum samples were thawed on ice at 4 °C for 30–60 min until no ice remained in the tubes. In total, 100 μL of serum was extracted with 600 μL of chloroform/methanol (3/1, v/v) by ultrasound for 1 h and mixed with 100 μL of water thoroughly. Then, 300 μL of the subnatant was centrifuged, dried and dissolved in 400 μL of isopropyl alcohol/acetonitrile (1/1, v/v) by ultrasound. The mixtures were centrifuged at 4 °C and 12,000 rpm for 10 min. After centrifugation, 100 μL of supernatant was carefully transferred to one 200 μL vial insert for analysis.

2.5. Biochemical analysis

Biochemical parameters including alanine aminotransferase (ALT), aspartate aminotransferase (AST), lactate dehydrogenase (LDH), creatine kinase (CK), calcium (Ca^{2+}), triglycerides (TG), total cholesterol (TCHO), high-density lipoprotein (HDL) and low-density lipoprotein (LDL), were measured using a direct method with a 7180 clinical analyzer (Hitachi High-technologies Corporation, Japan).

2.6. The UPLC-MS method

Metabolomics was performed with ultra-high-performance liquid chromatography (UPLC, Waters Corp., Milford, MA, USA) coupled with a hybrid quadrupole-orbitrap mass spectrometer (Thermo Scientific, San Jose, CA, USA). Chromatographic separation was employed with an HSST3 C_{18} column (2.1 × 100 mm, 1.7 μm, Waters) at 50 °C. Mobile phase A was acetonitrile/water (60/40, v/v) and mobile phase B was

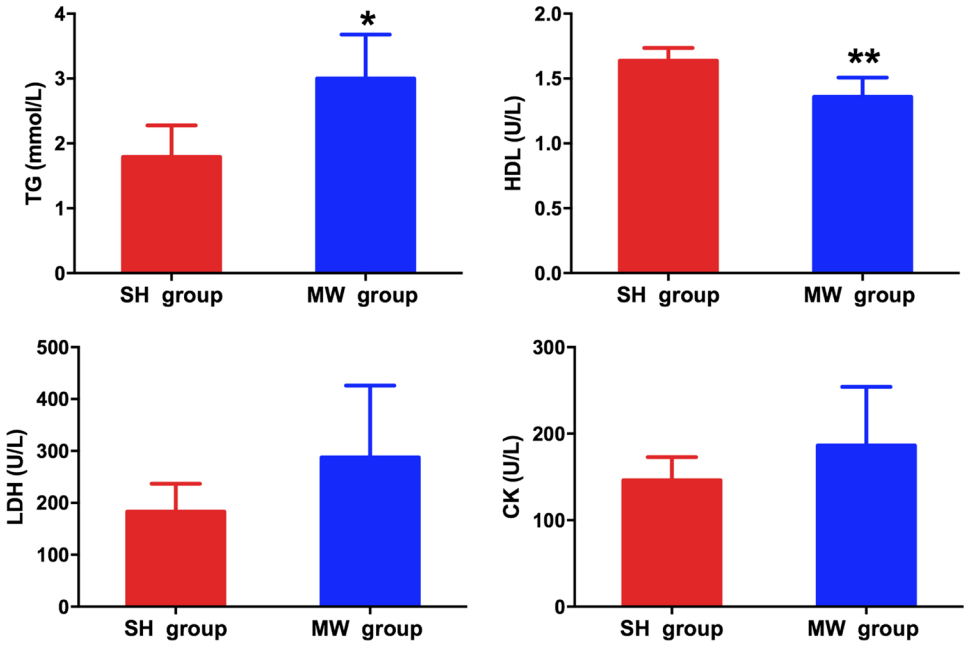

Fig. 2. Alterations of serum biochemical parameters in rats after microwave exposure 7d. Data was shown as mean ± SD, * $P < 0.05$, ** $P < 0.01$, compared with SH group.

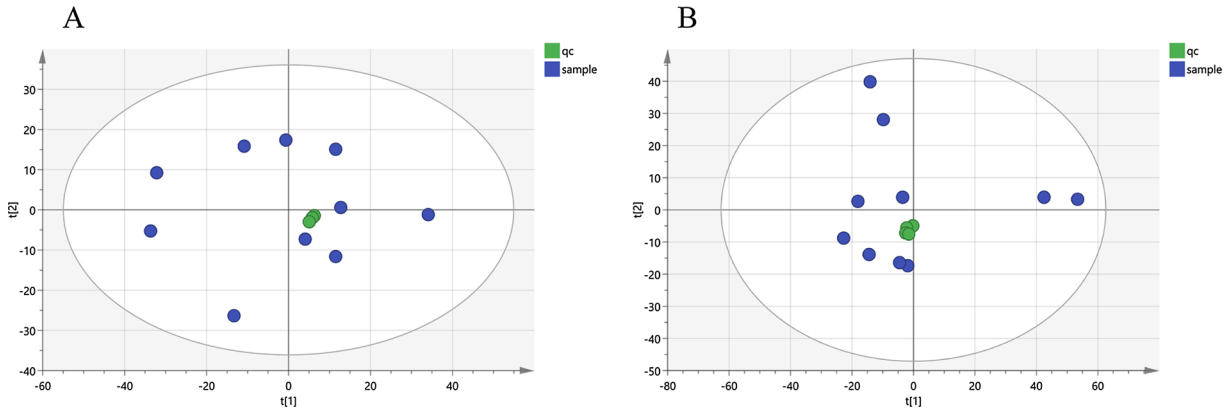

Fig. 3. PCA score plots. Overview of PCA score plots obtained from samples of microwave radiation group and sham group (blue), and QC samples (green) in positive ion mode (3A) and negative ion mode (3B).

isopropanol/acetonitrile (90/10, v/v); both A and B contained 0.1% formic acid and 10 mmol/L ammonium acetate. The flow rate was 0.3 mL/min, and the injection volume was 1 μL. The initial elution was started at 20% B for 1 min and immediately increased by a linear gradient to 100% B within 10 min. Over the next 8 min, the gradient was 100% B. Finally, 100% B returned to 20% over the next 0.5 min and equilibrated for 5 min for the next injection.

Both positive and negative ion modes were performed and operated. The positive and negative HESI-II spray voltages were 3.7 kV and 3.5 kV, respectively. The heated capillary temperature was 320 °C; the sheath gas pressure was 30 psi; the auxiliary gas setting was 10 psi; and the heated vaporizer temperature was 300 °C. The sheath gas and the auxiliary gas were both nitrogen. The collision gas was also nitrogen at a pressure of 1.5 mTorr. The parameters of the full mass scan were as follows: a resolution of 70,000, an auto gain control target under 1×10^6, a maximum isolation time of 50 ms and a mass-to-charge (m/z) range of 150–1500.

2.7. Data processing and statistical analysis

All of the MS data were processed using Progenesis QI software (Nonlinear Dynamics, Newcastle, UK) for imputing raw data, peak alignment, picking, and normalization to produce peak intensities for retention time (t_R) and mass-to-charge ratio (m/z) data pairs (Dong et al., 2018). The range of automatic peak picking was between 0.7 and 19 min.

Multivariate analysis was performed using SIMCA14.1 software (Umetrics AB, Umea, Sweden) (Wheelock and Wheelock, 2013). A principal component analysis (PCA) was used as an unsupervised method for data visualization and outlier identification. An orthogonal partial least squares discriminant analysis (OPLS-DA) was further applied to identify the potential biomarkers. The biomarkers were filtered and confirmed by combining the results of the variable importance in the projection (VIP) values (VIP > 1) and *t-test* ($p < 0.05$). The R^2 and Q^2 values can explain the quality of the fitting of the model.

The 760 peaks of positive ion mode and 1585 peaks of negative ion mode were detected according to the UPLC-MS data. Based on the VIP value of OPLS-DA (VIP > 1) and the p value of the *t-test* ($p < 0.05$), 68 different lipid metabolites were chosen and identified by their retention time, MS data and the characteristic fragment of MS or the tandem mass fragment of MS^2. Furthermore, the databases, including a self-built database of more than 600 metabolite standards and available

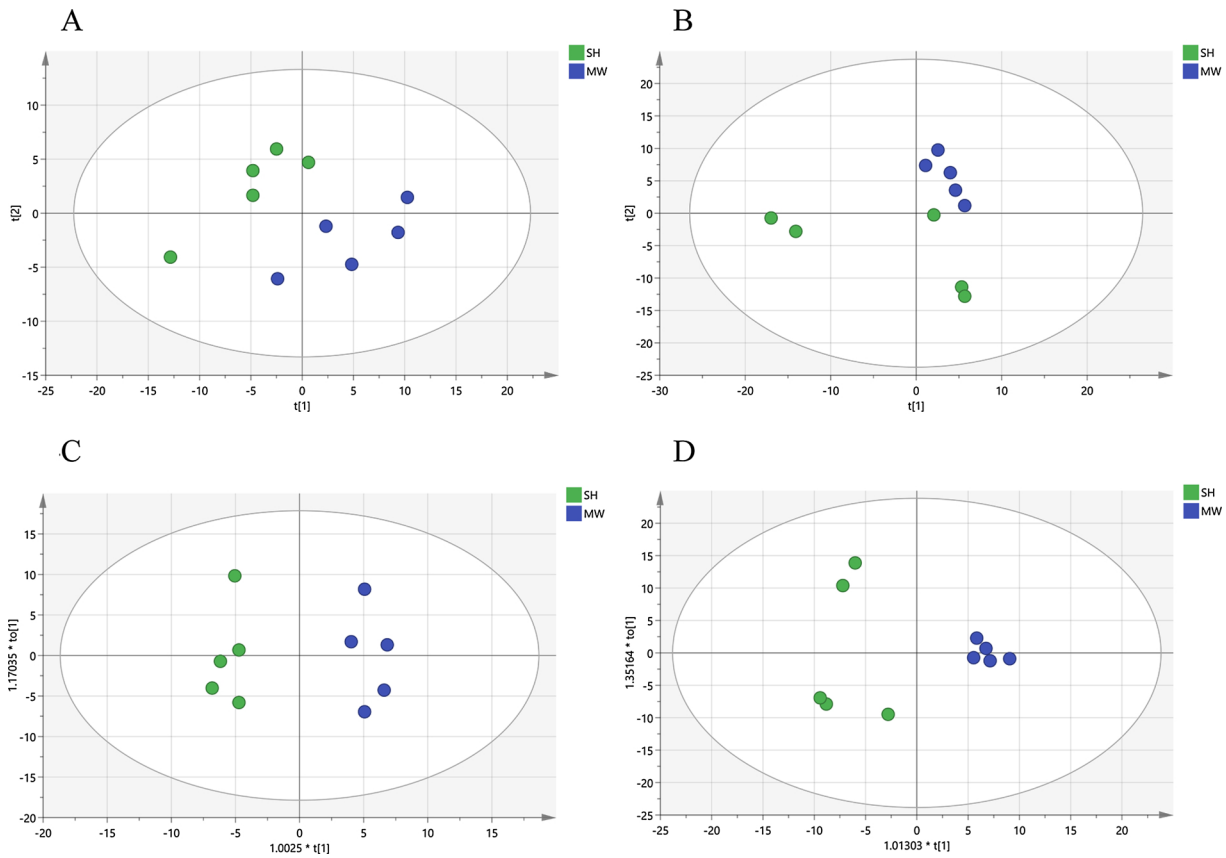

Fig. 4. PCA and OPLS-DA score plots from microwave radiation group and sham group. (4A) PCA score plot in positive ion mode (R2X = 0.728, Q2 = 0.546). (4B) PCA score plot in negative ion mode (R2X = 0.610, Q2 = 0.290). (4C) OPLS-DA score plot in positive ion mode (R2Y = 0.995, Q2 = 0.950). (4D) OPLS-DA score plot in negative ion mode (R2Y = 0.929, Q2 = 0.776).

databases such as HMDB (http://www.hmdb.ca/) and LIPID MAPS (http://www.Lipidmaps.org/tools/index.html), were used for verification and identification. For example, in positive ion mode, the ions of *m/z* 780.5524 (t_R, 10.04 min) and 992.7681 (t_R, 16.73 min) were speculated as $C_{44}H_{78}NO_8P$ and $C_{65}H_{98}O_6$, respectively, by analyzing the elemental composition and the fractional isotope abundance. Then, the two metabolites were identified as PC (20:4_16:1) and TG (18:2_22:6_22:6) after comparing characteristic fragments of PC (20:4_16:1) (303 and 253) in negative ion mode and tandem mass fragments of MS^2 of TG (18:2_22:6_22:6) (647 and 695) in positive ion mode with HMDB and LIPID MAPS databases.

Serum biochemistry data and AEL of the MWM were expressed as the mean ± the standard deviation (SD). Statistical significance was analyzed by unpaired *t*-tests using GraphPad Prism version 5.0 (GraphPad Software, San Diego, CA, USA).

3. Results

3.1. Effect of microwave radiation on cognitive function

Compared to the MW group, the rats in the SH group spent less time finding the submerged platform. However, rats in the MW group were unable to retrieve the location of the submerged platform that was learned during the training days, with longer AEL than the SH group ($p < 0.05$) after 14 d of microwave exposure (Fig. 1). Therefore, the data suggested that microwave radiation could cause cognitive injury.

3.2. Effect of microwave radiation on serum biochemistry

To illuminate the change in biochemical parameters, we tested the contents of serum Ca^{2+}, CK, LDH, AST, TCHO, TG, HDL and LDL at 6 h, 7 d, and 14 d after microwave radiation by an automatic blood chemistry analyzer, respectively. These data suggested that the serum biochemistry changed mainly 7 d after microwave radiation compared with the SH group. The biochemical parameters that increased were CK, LDH and TG ($p < 0.05$), and the parameter that decreased was HDL ($p < 0.01$), as shown in Fig. 2. Among them, our research found differences in TG and HDL levels between the SH group and the MW group for the first time, which further prompted us to study the feature of lipid metabolism related to microwave radiation.

3.3. Serum lipid profiling analysis of the MW group and the SH group

To investigate and understand the lipid metabolic alterations induced by microwave radiation, we first analyzed the differential lipids between the MW group and the SH group. We detected features in positive and negative ion modes eliminating the features in QC samples with coefficients of variation (CVs) over 15%, respectively. A PCA with QC samples was performed to assess the experiment quality. The PCA showed that the pooled QC samples were clustered together in both ion modes (positive and negative) (Fig. 3A and B), indicating that the process of UPLC-MS analysis met the required qualifications and deserved further research. Then, the PCA was performed on the data of the SH group and the MW group to evaluate their separation, and the PCA scores plot showed significant differences between the two groups. These results were further confirmed by a supervised method, such as OPLS-DA in which both groups were perfectly discriminated.

3.4. Identification of different lipid metabolites and pathways

To investigate the lipid metabolic variations, a PCA was used to analyze all observations initially acquired. The SH group and the MW

Table 1
Identification of differentially expressed lipid metabolites between sham group and microwave radiation group under ESI^+ and ESI^- scan.

No.	Metabolites	m/z	VIP Value	Fold change	p Value	Retention Time (min)	Ion mode
1	PC(16:0_18:1)	804.5763	1.373	1.449	0.0012	10.66	ESI^-
2	PC(18:1_16:0)	760.5838	1.202	1.522	0.0024	11.85	ESI^+
3	PC(16:1_16:0)	732.5525	1.407	1.930	0.0172	10.68	ESI^+
		776.5452	1.753	1.922	0.0080	9.98	ESI^-
4	PC(P-18:0_18:1)	816.6137	1.112	1.328	0.0096	11.39	ESI^-
5	PC(P-18:0_20:4)	794.6051	1.098	1.426	0.0016	12.74	ESI^+
		838.5971	1.526	1.745	0.0083	11.04	ESI^-
6	PC(P-18:0_20:5)	792.5886	1.073	1.403	0.0108	11.16	ESI^+
		836.5810	1.198	1.467	0.0176	10.25	ESI^-
7	PC(18:2_15:0)	744.5534	1.196	1.545	0.0390	12.74	ESI^+
8	PC(18:3_16:0)	800.5450	1.224	1.374	0.0384	9.71	ESI^-
9	PC(20:4_16:1)	780.5524	1.276	1.668	0.0198	10.04	ESI^+
10	PC(20:0_18:1)	816.6467	1.019	1.348	0.0009	14.69	ESI^+
11	LysoPC(16:1)	494.3237	1.180	1.610	0.0115	2.49	ESI^+
		538.3150	1.553	1.656	0.0063	7.27	ESI^-
12	LysoPC(18:2)	564.3305	1.367	1.433	0.0346	7.43	ESI^-
13	LysoPC(18:3)	518.324	1.493	1.937	0.0004	2.30	ESI^+
		562.3151	1.369	1.541	0.0004	7.21	ESI^-
14	LysoPC(20:2)	548.3708	1.336	1.652	0.0097	4.32	ESI^+
15	LysoPC(20:3)	546.3552	1.199	1.486	0.0003	3.39	ESI^+
		590.3464	1.239	1.358	0.0341	7.62	ESI^-
16	LysoPC(20:5)	542.3238	1.593	2.104	0.0005	2.15	ESI^+
		586.3152	1.822	2.118	0.0003	7.20	ESI^-
17	LysoPC(22:5)	570.3551	1.107	1.524	0.0167	3.07	ESI^+
18	PE(16:0_18:1)	716.524	1.552	1.768	0.0492	10.66	ESI^-
19	PE(P-18:0_18:2)	726.5452	1.007	1.315	0.0116	11.37	ESI^-
20	PE(18:1_18:0)	744.5545	1.408	1.482	0.0022	10.66	ESI^-
21	PE(18:2_16:0)	714.5084	1.466	1.753	0.0346	10.19	ESI^-
22	PE(20:4_16:0)	740.5216	1.029	1.439	0.0407	11.15	ESI^+
23	PE(20:4_18:0)	766.5382	1.456	1.564	0.0225	9.89	ESI^-
24	PE(22:6_16:0)	762.5083	2.224	2.954	0.0214	10.06	ESI^-
25	LysoPE(0:0_16:0)	452.2782	1.680	1.728	0.0098	7.48	ESI^-
26	LysoPE(0:0_18:0)	480.3094	1.177	1.354	0.0291	7.88	ESI^-
27	LysoPE(0:0_18:1)	478.2939	1.464	1.699	0.0136	7.14	ESI^-
28	LysoPE(0:0_20:2)	504.3096	1.470	1.531	0.0101	7.32	ESI^-
29	LysoPE(16:0_0:0)	454.2925	1.244	1.580	0.0016	3.71	ESI^+
		452.2781	1.515	1.588	0.0067	7.60	ESI^-
30	LysoPE(16:1_0:0)	450.2625	2.228	2.635	0.0064	7.28	ESI^-
31	LysoPE(18:0_0:0)	480.3093	1.152	1.370	0.0116	7.98	ESI^-
32	LysoPE(18:1_0:0)	478.2938	1.572	1.715	0.0077	7.27	ESI^-
33	LysoPE(20:2_0:0)	504.3096	1.373	1.437	0.0380	7.43	ESI^-
34	PI(16:0_18:1)	835.5352	1.011	1.243	0.0209	9.66	ESI^-
35	PI(16:0_18:2)	833.5193	1.049	1.289	0.0168	9.34	ESI^-
36	TG(14:0_16:0_16:1)	794.7221	2.760	7.917	0.0007	17.25	ESI^+
37	TG(14:0_18:0_16:0)	824.7691	1.258	1.647	0.0136	17.77	ESI^+
38	TG(14:0_18:1_16:0)	822.7533	2.077	3.424	0.0004	17.52	ESI^+
39	TG(15:0_18:1_16:0)	836.7692	1.650	2.238	0.0018	17.66	ESI^+
40	TG(15:0_18:1_18:2)	860.7689	1.409	1.786	0.0047	17.43	ESI^+
41	TG(16:0_14:0_16:0)	796.7377	1.262	1.717	0.0129	17.51	ESI^+
42	TG(16:0_15:0_18:0)	838.7848	1.408	1.871	0.0117	17.91	ESI^+
43	TG(16:0_16:0_18:0)	852.8003	1.276	1.689	0.0245	18.04	ESI^+
44	TG(16:0_16:1_14:1)	792.7062	2.131	3.808	0.0009	16.99	ESI^+
45	TG(16:0_16:1_18:1)	848.769	1.666	2.163	0.0002	17.54	ESI^+
46	TG(16:0_16:1_18:2)	846.7533	1.802	2.473	0.0005	17.29	ESI^+
47	TG(16:0_18:0_18:1)	878.8159	1.509	2.036	0.0060	18.04	ESI^+
48	TG(16:0_18:1_16:0)	850.7846	1.651	2.181	0.0007	17.78	ESI^+
49	TG(16:0_18:2_16:0)	848.7694	2.513	5.996	0.0016	18.21	ESI^+
50	TG(16:1_14:0_18:1)	820.7376	2.056	3.321	0.0004	17.28	ESI^+
51	TG(16:1_14:0_18:2)	818.7218	1.995	3.122	0.0012	17.01	ESI^+
52	TG(16:1_15:0_18:2)	832.7376	1.749	2.405	0.0023	17.17	ESI^+
53	TG(18:1_16:0_18:1)	876.8001	1.528	1.907	0.0003	17.79	ESI^+
54	TG(18:1_22:4_22:6)	998.8152	2.156	3.825	0.0053	17.27	ESI^+
55	TG(18:2_20:5_22:5)	968.7684	1.209	1.568	0.0027	16.84	ESI^+
56	TG(18:2_22:5_22:6)	994.7838	1.617	2.197	0.0077	16.83	ESI^+
57	TG(18:2_22:6_22:6)	992.7681	1.680	2.239	0.0008	16.73	ESI^+
58	TG(18:3_22:6_22:6)	990.7533	1.744	2.465	0.0044	16.53	ESI^+
59	TG(22:4_18:2_22:6)	996.7998	1.769	2.502	0.0056	17.05	ESI^+
60	SM(d18:1_24:1)	813.6830	1.052	1.372	0.0012	14.72	ESI^+
61	CE(22:6)	714.6174	2.031	2.986	0.0121	17.81	ESI^+
62	9,10-DHOME	313.2387	1.315	1.505	0.0113	6.52	ESI^-
63	Ethyl 3-hydroxydodecanoate	243.1964	1.165	1.340	0.0277	6.79	ESI^-
64	(R)-2-Hydroxyhexadecanoic acid	271.2280	1.100	1.302	0.0185	6.84	ESI^-
65	5,8-Tetradecadienoic acid	223.1698	1.241	1.441	0.0002	7.06	ESI^-
66	Linoleic acid	279.2327	1.060	1.273	0.0206	7.33	ESI^-

(*continued on next page*)

Table 1 (*continued*)

No.	Metabolites	m/z	VIP Value	Fold change	p Value	Retention Time (min)	Ion mode
67	Homophytanic acid	325.3113	1.139	1.496	0.0168	9.30	ESI^-
68	Nervonic acid	365.3423	1.019	1.522	0.0375	9.82	ESI^-

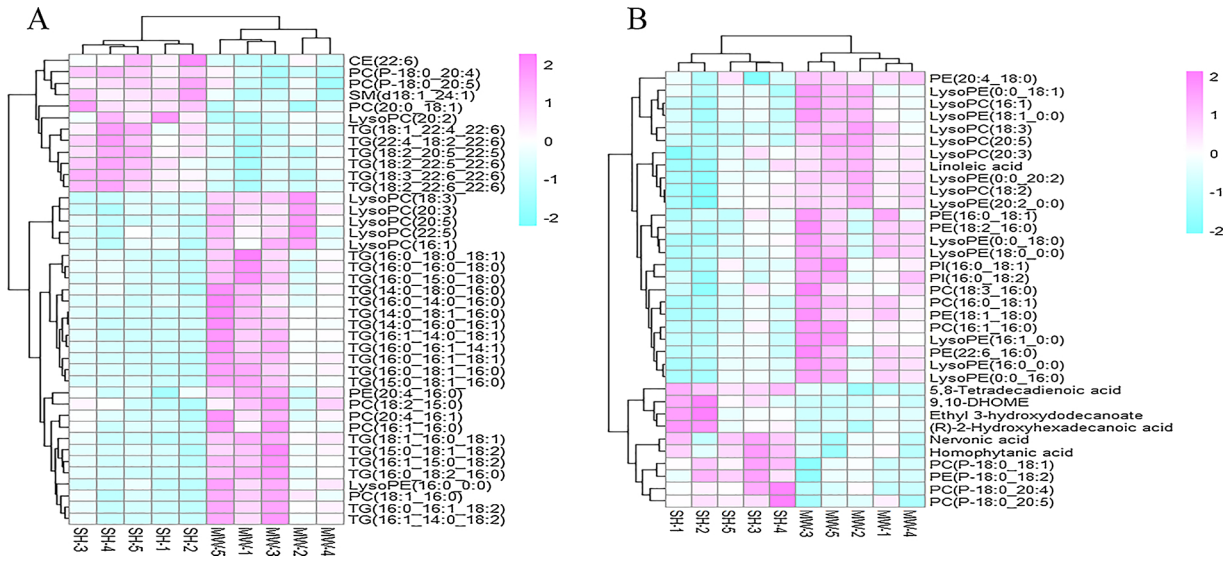

Fig. 5. Heatmap of the differential expressed lipid metabolites. (5A) positive ion mode, and (5B) negative ion mode. The color is proportional to the intensity of change in metabolites; red indicates up-regulation and blue indicates down-regulation.

group exhibited an improved separation, as shown in Fig. 4A (positive, $R^2X = 0.728$, $Q^2 = 0.0546$) and Fig. 4B (negative, $R^2X = 0.610$, $Q^2 = 0.290$). Next, OPLS-DA was applied to compare the lipid changes in the two groups. The model showed excellent predictive power by monitoring the model of the goodness of fit (R^2Y) and predictive ability (Q^2) values, as shown in Fig. 4C (positive, $R^2Y = 0.995$, $Q^2 = 0.950$) and Fig. 4D (negative, $R^2Y = 0.929$, $Q^2 = 0.776$). Based on the VIP value of OPLS-DA and the p value of the *t*-test, the criteria of VIP > 1 and $p < 0.05$ were set to discover significantly different features (33 in positive ion mode, 27 in negative ion mode and 8 in both modes). Finally, 68 endogenous lipids in the serum were identified by comparing their MS data with a self-built database of more than 600 metabolite standards and available databases such as HMDB (http://www.hmdb.ca/) and LIPID MAPS (http://www.Lipidmaps.org/tools/index.html), which were differentially expressed between the MW group and SH group (Table 1). The identified lipids belong to different lipid classes, mainly including the phosphatidylcholine (PC), lysophosphatidylcholine (LPC), phosphatidylethanolamine (PE), lysophosphatidylethanolamine (LPE), triacylglycerol (TG) and free fatty acid (FFA) classes.

The heatmaps exhibited the differential expression of each lipid (Fig. 5A and B). According to our results, the levels of PEs, LPEs, LPCs, PIs and linoleic acid were mainly upregulated, while sphingomyelin (SM), cholesterol esters (CE) and the other FFAs were downregulated. PCs and TGs increased or decreased. These alterations in endogenous lipids were well matched with the changes in serum TG and HDL in microwave-exposed rats.

Furthermore, a metabolic pathway map was constructed based on the MataboAnalyst program (http://www.MataboAnalyst.ca/). The important lipid metabolic pathways were involved in linoleic acid metabolism, glycerophospholipid metabolism, glycerolipid metabolism and glycosylphosphatidylinositol (GPI)-anchor biosynthesis (Fig. 6A). The above-identified differential lipid metabolites were finally connected to different pathways, and the lipid metabolic networks were structured as shown in Fig. 6B.

4. Discussion

The brain is one of the most sensitive targets for microwave radiation and, meanwhile, raises many concerns. Accumulating evidence has demonstrated that microwave radiation results in memory impairment, including the damage of hippocampal structures, the decrease in neurotransmitters and the decrease in the number of synaptic vesicles in rats (Hao et al., 2015). However, the changes in behavior and cognition are essential to assess the effects of microwave radiation on the brain. In this study, we found the microwave radiation produced marked alterations in the function of the brain by MWM tests, which not only established an available model of microwave radiation but also provided a crucial clue concerning cognitive damage and abnormal metabolism of lipids caused by microwave radiation.

Interestingly, the results of the present study first revealed a close relationship between microwave radiation and lipid metabolism, including the identification of differentially expressed lipids and analysis of lipid metabolic pathways. Lipids, as a significant class of molecules, have played an increasingly recognized role in the maintenance of neuronal function in the brain. Brain lipids determine the localization and function of proteins in the cell membrane of neurons (Schneider et al., 2017). Lipids may also act as barriers and neurotransmitters or other signaling media to regulate the membrane's function and synaptic throughput (Müller et al., 2015). Thus, the changes in the lipid metabolic pathway may be one of the mechanisms of cognitive damage by microwave radiation, which has not been focused on before.

In the lipid metabolic networks, PCs were the essential lipid classe possessing more connections with PEs, LPEs, LPCs, TGs and FFAs through the four abovementioned main metabolic pathways. PC comprises 40–50% of total cellular phospholipids, both the critical components of the cellular lipid bilayer and the nuclear receptor of peroxisome proliferator-activated receptors (PPARs), which can govern the lipid metabolism, primarily regulating lipid, lipoprotein and whole-body energy metabolism (Xu et al., 2017). Therefore, people pay it more attention compared with health and diseases (van der Veen et al.,

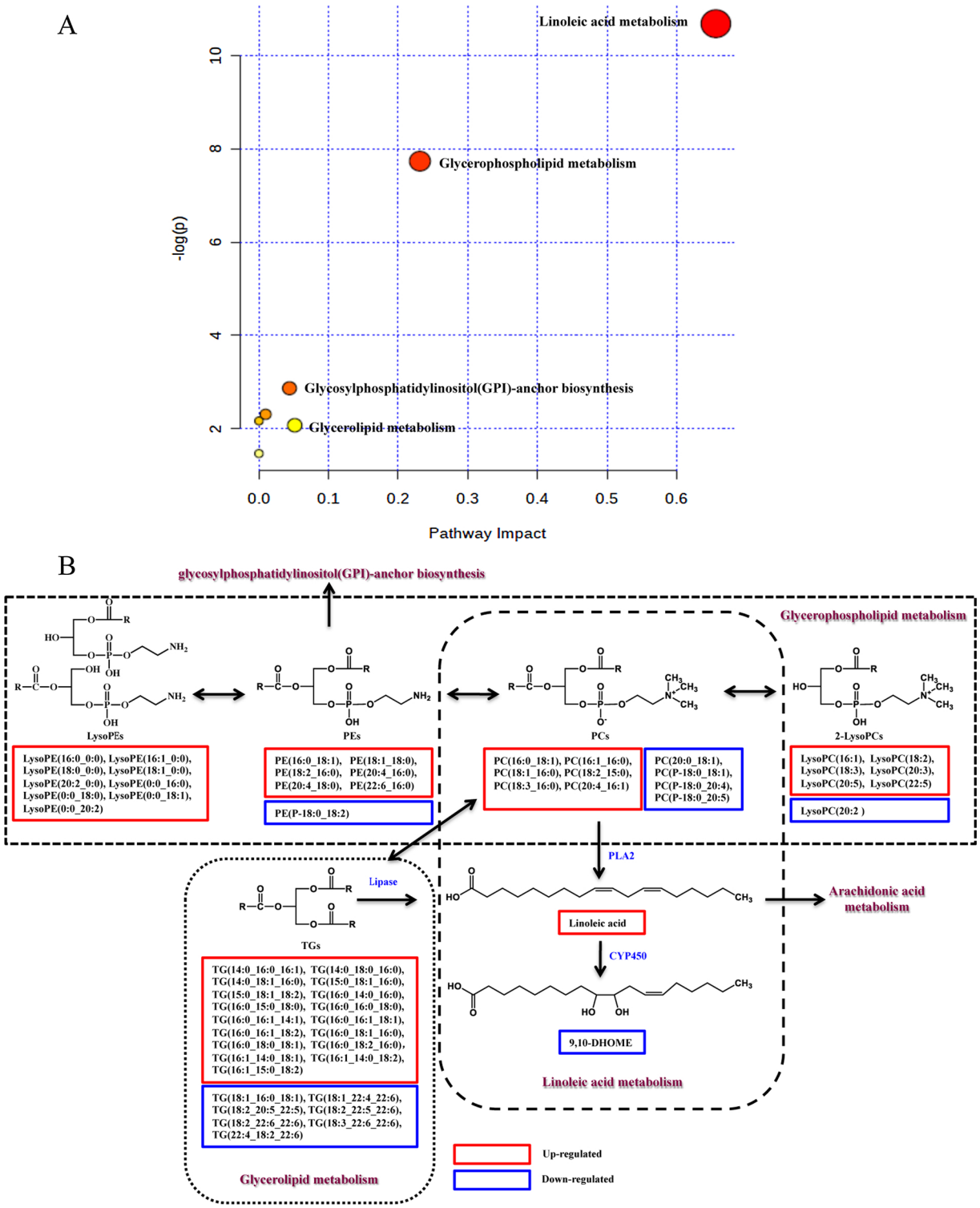

Fig. 6. Analysis of lipid metabolic pathways induced by microwave radiation. (6A) Summary of pathways with Metaboanalyst. (6B) Important network of lipid metabolic pathways caused by microwave exposure.

2017), such as cystic fibrosis (Grothe et al., 2015), atherosclerosis (Dang et al., 2016), autoimmune hepatitis (Zhou et al., 2016) and cancer (Bao et al., 2016). Moreover, PCs are involved in nervous system protection. The occurrence of choline in the structure of the PC helps to increase the choline levels in the nervous system, and its anti-inflammatory action could be PC's primary mechanism (Tayebati, 2018). Our present study proposed that the concentrations of 6 PCs with two usual chains of FAs exhibited an increase in the MW group, while 3 ether PCs consisting of one chain of plasmalogen 18:0 at the C-1 position were decreased significantly. Plasmalogens are particular glycerol ether phospholipids enriched in the nervous system. In the animal models of the nervous system, ether phospholipids are deficient, which highlights their potential roles in neurological diseases involved in Alzheimer's disease. Moreover, the drugs to restore ether phospholipids create additional interest in treatment strategy (Dorninger et al., 2017). Thus, the decline in three ether PCs in the MW group may be linked to

lipid metabolism disorders and, especially, to memory impairment induced by microwave radiation.

In this study, linoleic acid metabolism showed the highest pathway impact, and a higher linoleic acid concentration was obtained in the MW group. Linoleic acid metabolism follows pathways regulated by LOX and CYP enzymes, of which the CYP pathway leads to 9,10-epoxyoctadecamonoenoic acid (9,10-EpOME), which is subsequently converted to 9,10-dihydroxyoctadecamonoenoic acid (9,10-DHOME) (Saccenti et al., 2015). Our results suggested that the level of 9,10-DHOME was decreased, and the level of linoleic acid increased, which exhibited the CYP pathway was significantly impeded in the MW group. Due to it being a precursor of arachidonic acid, a majority of studies indicated that linoleic acid and its derivatives were able to demonstrate a direct/indirect correlation with inflammation and metabolic diseases (Choque et al., 2014). Clouard et al. (2015) reported that low intake of linoleic acid contributed to increased exploration and decreased anxiety-related behavior in pigs. Additionally, evidence has shown that linoleic acid is strongly associated with Alzheimer's disease and mild cognitive impairment (Brayne et al., 2017; Wang et al., 2014a). Except for linoleic acid, we found five other FFAs' levels declined markedly in the MW group, which might be related to the hampering of the lipase pathway. Among these decreased FFAs, nervonic acid is an essential molecule for the growth and maintenance of the brain and peripheral nervous tissue. Furthermore, nervonic acid in the plasma has been certified as a potential biomarker for major depressive disorder (Kageyama et al., 2018). Although the levels of linoleic acid and nervonic acid in previous reports conflicted with our results, which might be due to differences in diseases, type of samples or time of detection, the disturbances of linoleic acid and nervonic acid in nervous system diseases were revealed and attracted interest.

TGs are also significant components and play an essential role in energy metabolism. Our results found that many TGs exhibited alterations due to microwave radiation involving glycerolipid metabolism. Importantly, 6 TGs with FA side chains exceeding 18 carbons showed downregulation, while 18 TGs consisting of FA side chains below 16 carbons exhibited upregulation. Furthermore, this metabolic pathway was closely related to linoleic acid metabolism and glycerophospholipid metabolism, further affecting the changes in PCs, TGs and FFAs. As a novel cellular signaling entity, glycerolipid-metabolizing enzymes present attractive targets for new therapies (Scott et al., 2014). However, there is a relative limitation of the effects of glycerolipid metabolism on diseases.

5. Conclusion

We expectedly demonstrated that microwave radiation could lead to disturbances in lipid metabolism. Therefore, we analyzed lipid metabolic changes between the SH group and the MW group for the first time. Based on untargeted metabolomics investigation, 68 disturbed lipids were identified mainly as PC, LPC, PE, LPE, TG and FFA, which were mainly involved in linoleic acid metabolism, glycerophospholipid metabolism, glycerolipid metabolism and glycosylphosphatidylinositol (GPI)-anchor biosynthesis. Our research on monitoring the changes in lipid metabolism could shed light on the metabolic mechanism of microwave radiation injury and provide a new strategy for the prevention of microwave radiation. Our results suggested that many different lipid metabolites, including PC and FFAs, were strongly linked to nervous system impairment, which was one of the most concerning biological effects caused by microwave radiation. Some researches has also supported that endogenous lipids are essential regulators of neural cell proliferation, differentiation, oxidative stress, inflammation and apoptosis (Farooqui, 2009). Therefore, our future studies will focus on the correlation between cognitive damage caused by microwave radiation and abnormal lipid metabolism, which will help to provide a new therapeutic strategy for microwave radiation injury. Moreover, the present study provided crucial information for future research.

Declaration of Competing Interest

The authors declare that they have no known competing financial interests or personal relationships that could have appeared to influence the work reported in this paper.

References

Adams, J.A., Galloway, T.S., Mondal, D., Esteves, S.C., Mathews, F., 2014. Effect of mobile telephones on sperm quality: a systematic review and meta-analysis. Environ. Int. 70, 106–112.

Bao, J., Liu, F., Zhang, C., Wang, K., Jia, X., Wang, X., Chen, M., Li, P., Su, H., Wang, Y., Wan, J.B., He, C., 2016. Anti-melanoma activity of *Forsythiae Fructus* aqueous extract in mice involves regulation of glycerophospholipid metabolisms by UPLC/Q-TOF MS-based metabolomics study. Sci. Rep. 6, 39415.

Brayne, C., Snowden, S.G., Ebshiana, A.A., Hye, A., An, Y., Pletnikova, O., O'Brien, R., Troncoso, J., Legido-Quigley, C., Thambisetty, M., 2017. Association between fatty acid metabolism in the brain and Alzheimer disease neuropathology and cognitive performance: a nontargeted metabolomic study. PLoS Med. 14, e1002266.

Chauhan, P., Verma, H.N., Sisodia, R., Kesari, K.K., 2017. Microwave radiation (2.45 GHz)-induced oxidative stress: whole-body exposure effect on histopathology of Wistar rats. Electromagn. Biol. Med. 36, 20–30.

Choque, B., Catheline, D., Rioux, V., Legrand, P., 2014. Linoleic acid: between doubts and certainties. Biochimie 96, 14–21.

Clouard, C., Gerrits, W.J.J., van Kerkhof, I., Smink, W., Bolhuis, J.E., 2015. Dietary linoleic and α-linolenic acids affect anxiety-related responses and exploratory activity in growing pigs. J. Nutr. 145, 358–364.

Dang, V.T., Huang, A., Zhong, L.H., Shi, Y., Werstuck, G.H., 2016. Comprehensive plasma metabolomic analyses of atherosclerotic progression reveal alterations in glycerophospholipid and sphingolipid metabolism in apolipoprotein e-deficient mice. Sci. Rep. 6, 35037.

Dong, S., Zhang, S., Chen, Z., Zhang, R., Tian, L., Cheng, L., Shang, F., Sun, J., 2018. Berberine could ameliorate cardiac dysfunction via interfering myocardial lipidomic profiles in the rat model of diabetic cardiomyopathy. Front. Physiol. 9, 1042.

Dorninger, F., Forss-Petter, S., Berger, J., 2017. From peroxisomal disorders to common neurodegenerative diseases—the role of ether phospholipids in the nervous system. FEBS Lett. 591, 2761–2788.

Farooqui, A.A., 2009. Lipid mediators in the neural cell nucleus: their metabolism, signaling, and association with neurological disorders. Neuroscientist 15, 392–407.

Grothe, J., Riethmüller, J., Tschürtz, S.M., Raith, M., Pynn, C.J., Stoll, D., Bernhard, W., 2015. Plasma phosphatidylcholine alterations in cystic fibrosis patients: impaired metabolism and correlation with lung function and inflammation. Cell. Physiol. Biochem. 35, 1437–1453.

Hao, Y.H., Zhao, L., Peng, R.Y., 2015. Effects of microwave radiation on brain energy metabolism and related mechanisms. Mil. Med. Res. 2, 4.

Hao, Y., Li, W., Wang, H., Zhang, J., Yu, C., Tan, S., Wang, H., Xu, X., Dong, J., Yao, B., Zhou, H., Zhao, L., Peng, R., 2018. Autophagy mediates the degradation of synaptic vesicles: a potential mechanism of synaptic plasticity injury induced by microwave exposure in rats. Physiol. Behav. 188, 119–127.

Hu, S., Peng, R., Wang, C., Wang, S., Gao, Y., Dong, J., Zhou, H., Su, Z., Qiao, S., Zhang, S., Wang, L., Wen, X., 2014. Neuroprotective effects of dietary supplement Kang-fuling against high-power microwave through antioxidant action. Food Funct. 5, 2243–2251.

Kageyama, Y., Kasahara, T., Nakamura, T., Hattori, K., Deguchi, Y., Tani, M., Kuroda, K., Yoshida, S., Goto, Y.-i., Inoue, K., Kato, T., 2018. Plasma nervonic acid is a potential biomarker for major depressive disorder: a pilot study. Int. J. Neuropsychopharmacol. 21, 207–215.

Kaplan, S., Deniz, O.G., Önger, M.E., Türkmen, A.P., Yurt, K.K., Aydın, I., Altunkaynak, B.Z., Davis, D., 2016. Electromagnetic field and brain development. J. Chem. Neuroanat. 75, 52–61.

Lewicka, M., Henrykowska, G., Zawadzka, M., Rutkowski, M., Pacholski, K., Buczyński, A., 2017. Impact of electromagnetic radiation emitted by monitors on changes in the cellular membrane structure and protective antioxidant effect of vitamin A—in vitro study. Int. J. Occup. Med. Environ. Health 30, 695–703.

Li, X., Wang, L.F., Peng, R.Y., Gao, Y.B., Xu, X.P., Wang, S.X., Li, Y., Zhao, L., Dong, J., Chang, G.M., 2011. Influence of microwave radiation on contents of amino acids and monoamines in the urine of rhesus monkeys. Mil. Med. Res. 35, 365–368.

Meena, R., Kumari, K., Kumar, J., Rajamani, P., Verma, H.N., Kesari, K.K., 2014. Therapeutic approaches of melatonin in microwave radiations-induced oxidative stress-mediated toxicity on male fertility pattern of Wistar rats. Electromagn. Biol. Med. 33, 81–91.

Müller, C.P., Reichel, M., Mühle, C., Rhein, C., Gulbins, E., Kornhuber, J., 2015. Brain membrane lipids in major depression and anxiety disorders. Biochim. Biophys. Acta 1851, 1052–1065.

Pall, M.L., 2016. Microwave frequency electromagnetic fields (EMFs) produce widespread neuropsychiatric effects including depression. J. Chem. Neuroanat. 75, 43–51.

Redlarski, G., Lewczuk, B., Zak, A., Koncicki, A., Krawczuk, M., Piechocki, J., Jakubiuk, K., Tojza, P., Jaworski, J., Ambroziak, D., Skarbek, L., Gradolewski, D., 2015. The influence of electromagnetic pollution on living organisms: historical trends and forecasting changes. BioMed Res. Int. 2015, 234098.

Saccenti, E., van Duynhoven, J., Jacobs, D.M., Smilde, A.K., Hoefsloot, H.C., 2015. Strategies for individual phenotyping of linoleic and arachidonic acid metabolism using an oral glucose tolerance test. PLoS One 10, e0119856.

Schneider, M., Levant, B., Reichel, M., Gulbins, E., Kornhuber, J., Müller, C.P., 2017. Lipids in psychiatric disorders and preventive medicine. Neurosci. Biobehav. Rev. 76, 336–362.
Scott, S.A., Mathews, T.P., Ivanova, P.T., Lindsley, C.W., Brown, H.A., 2014. Chemical modulation of glycerolipid signaling and metabolic pathways. Biochim. Biophys. Acta 1841, 1060–1084.
Tayebati, S., 2018. Phospholipid and lipid derivatives as potential neuroprotective compounds. Molecules 23, 2257.
van der Veen, J.N., Kennelly, J.P., Wan, S., Vance, J.E., Vance, D.E., Jacobs, R.L., 2017. The critical role of phosphatidylcholine and phosphatidylethanolamine metabolism in health and disease. Biochim. Biophys. Acta 1859, 1558–1572.
Wang, L.F., Li, X., Peng, R.Y., Gao, Y.B., Zhao, L., Wang, S.M., Xu, X.P., Dong, J., Li, Y., Wang, S.X., 2011. A metabolomic approach to screening urinary metabolites upon microwave exposure in monkeys. Mil. Med. Res. 35, 369–378.
Wang, G., Zhou, Y., Huang, F.J., Tang, H.D., Xu, X.H., Liu, J.J., Wang, Y., Deng, Y.L., Ren, R.J., Xu, W., Ma, J.F., Zhang, Y.N., Zhao, A.H., Chen, S.D., Jia, W., 2014a. Plasma metabolite profiles of Alzheimer's disease and mild cognitive impairment. J. Proteome Res. 13, 2649–2658.
Wang, L., Li, X., Gao, Y., Wang, S., Zhao, L., Dong, J., Yao, B., Xu, X., Chang, G., Zhou, H., Hu, X., Peng, R., 2014b. Activation of VEGF/FLK-1-ERK pathway induced blood–-brain barrier injury after microwave exposure. Mol. Neurobiol. 52, 478–491.
Wheelock, Å.M., Wheelock, C.E., 2013. Trials and tribulations of 'omics data analysis: assessing quality of SIMCA-based multivariate models using examples from pulmonary medicine. Mol. Biosyst. 9.
Xu, J., Tang, L., Zhang, Q., Wei, J., Xian, M., Zhao, Y., Jia, Q., Li, X., Zhang, Y., Zhao, Y., Wu, H., Yang, H., 2017. Relative quantification of neuronal polar lipids by UPLC-MS reveals the brain protection mechanism of Danhong injection. RSC Adv. 7, 45746–45756.
Yuksel, M., Naziroglu, M., Ozkaya, M.O., 2016. Long-term exposure to electromagnetic radiation from mobile phones and Wi-Fi devices decreases plasma prolactin, progesterone, and estrogen levels but increases uterine oxidative stress in pregnant rats and their offspring. Endocrine 52, 352–362.
Zhang, J., Zhang, B., Wang, H., Xu, X.P., Yao, B.W., Zhao, L., Dong, J., Wang, H.Y., Peng, R.Y., 2017. Quantitative studies on the biological long-term effects of heart injury in rats induced by microwave radiation. Chin. J. Stereol. Image Anal. 22, 1–9.
Zhao, Y.Y., Lin, R.C., 2014. UPLC-MS(E) application in disease biomarker discovery: the discoveries in proteomics to metabolomics. Chem. Biol. Interact. 215, 7–16.
Zhao, L., Peng, R.Y., Wang, S.M., Wang, L.F., Gao, Y.B., Dong, J., Li, X., Su, Z.T., 2012a. Relationship between cognition function and hippocampus structure after long-term microwave exposure. Biomed. Environ. Sci. 25, 182–188.
Zhao, Y.-Y., Liu, J., Cheng, X.-L., Bai, X., Lin, R.-C., 2012b. Urinary metabonomics study on biochemical changes in an experimental model of chronic renal failure by adenine based on UPLC Q-TOF/MS. Clin. Chim. Acta 413, 642–649.
Zhao, Y.Y., Cheng, X.L., Wei, F., Bai, X., Tan, X.J., Lin, R.C., Mei, Q., 2013a. Intrarenal metabolomic investigation of chronic kidney disease and its TGF-beta1 mechanism in induced-adenine rats using UPLC Q-TOF/HSMS/MS(E). J. Proteome Res. 12, 692–703.
Zhao, Y.Y., Lei, P., Chen, D.Q., Feng, Y.L., Bai, X., 2013b. Renal metabolic profiling of early renal injury and renoprotective effects of Poria cocos epidermis using UPLC Q-TOF/HSMS/MSE. J. Pharm. Biomed. Anal. 81–82, 202–209.
Zhao, L., Yang, Y.-F., Gao, Y.-B., Wang, S.-M., Wang, L.-F., Zuo, H.-Y., Dong, J., Xu, X.-P., Su, Z.-T., Zhou, H.-M., Zhu, L.-L., Peng, R.-Y., 2014. Upregulation of HIF-1α via activation of ERK and PI3K pathway mediated protective response to microwave-induced mitochondrial injury in neuron-like cells. Mol. Neurobiol. 50, 1024–1034.
Zhou, C., Jia, H.M., Liu, Y.T., Yu, M., Chang, X., Ba, Y.M., Zou, Z.M., 2016. Metabolism of glycerophospholipid, bile acid and retinol is correlated with the early outcomes of autoimmune hepatitis. Mol. Biosyst. 12, 1574–1585.
Zuo, H., Lin, T., Wang, D., Peng, R., Wang, S., Gao, Y., Xu, X., Li, Y., Wang, S., Zhao, L., Wang, L., Zhou, H., 2014a. Neural cell apoptosis induced by microwave exposure through mitochondria-dependent caspase-3 pathway. Int. J. Med. Sci. 11, 426–435.
Zuo, H., Lin, T., Wang, D., Peng, R., Wang, S., Gao, Y., Xu, X., Zhao, L., Wang, S., Su, Z., 2014b. RKIP regulates neural cell apoptosis induced by exposure to microwave radiation partly through the MEK/ERK/CREB pathway. Mol. Neurobiol. 51, 1520–1529.